First developments of sub-micronic waveguide structures on UV210 polymer

D. Duval, C. Godet, N. Huby and B. Bêche
Institute of Physics
UMR CNRS 6251
Rennes, France
daphne.duval@univ-rennes1.fr

H. Lhermite
Institute of Electronics and Telecommunications
UMR CNRS 6164
Rennes, France

***Abstract*— First developments of sub-micronic waveguide structures on UV210 polymer are presented. The UV210 refractive index increases with exposure to DUV light ($\Delta n=2.10^{-2}$). Propagation losses are performed by a cut-back method in single-mode UV210 waveguides: values as low as 3.4 and 6.2 dB/cm are obtained for, respectively, TE_{00} and TM_{00} polarizations.**

Integrated optics; polymer rib waveguides; UV210 photo-resist; DUV lithography

I. Introduction

Over the last decades the use of polymers in integrated optics has been widely developed for the fabrication of low-cost devices such as sensors or optical telecommunication systems [1, 2]. However, as most photo-resists require classical lithographic processes within a 365 nm exposure wavelength, the resolution can be hardly better than 1 µm. Higher resolution can be obtained by using deep ultraviolet (DUV) lithography [3] on photo-resists such as the UV210 polymer. Moreover, exposure to DUV light can cause a variation of the refractive index of some polymers [4]. The interest of the UV210 resist has already been demonstrated in micro- / nano-electronic applications [5] but any use for photonic applications has been reported yet. The goal of this paper is to demonstrate the interest of the UV210 photo-resist for applications in integrated optics. At first, the study of the influence of DUV irradiation dose on the refractive index of the UV210 film is leaded by spectroscopic ellipsometry. Then, the photonic structure fabrication is described. Finally, optical losses at λ = 980 nm are measured for both TE_{00} and TM_{00} polarizations.

II. Photo-induced index variation in UV210 films

In order to study the variation of the UV210 refractive index as a function of the DUV irradiation dose, ellipsometric measurements (*Jobin Yvon-Horiba*) were carried out on as deposited UV210 film and on UV210 films exposed to DUV energy doses ranging from E = 20 mJ/cm^2 to E = 30 J/cm^2. The ellipsometric parameter $\rho = \tan(\psi).\exp(j\Delta)$ is inferred from the conventional ellipsometric angles ψ and Δ. The refractive index n of the UV210 film, spin-coated on silicon wafer, is obtained from a 3-layer model (Si-UV210-air) using an absorbing Cauchy dispersion law. As a result, n at λ = 980 nm is plotted as a function of the DUV irradiation doses on Fig. 1. Such as deposited UV210 film (E = 0 J/cm^2) has a refractive index of 1.565 at 980 nm. This value increases with the irradiation dose: for an exposure of 15 J/cm^2, we measure an enhancement of 2.10^{-2} in the refractive index value. For higher irradiation doses, the refractive index appears to remain constant. Thus, the following study will be limited to irradiation doses ranging from 20 mJ/cm^2 to 15 J/cm^2.

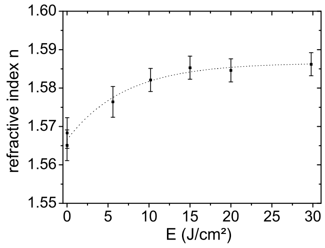

Figure 1. Refractive index values at λ = 980 nm as a function of DUV irradiation doses.

III. Fabrication processes

The UV210 being a positive photo-resist, the UV-exposed part of the resist is dissolved during the development step. Thus, two different optical microstructures have been realized: structures of family 1 consist of as deposited UV210 waveguides while for family 2, UV210 waveguides have been exposed to DUV light after the development step in order to study the influence of DUV-induced modifications on the polymer optical properties. Both families consist of UV210 rib waveguides on a (1 0 0) silicon substrate. A SiO_2 layer is first obtained by thermal oxidation of the silicon wafer yielding a 1.2 µm-thick layer (n_{SiO2}=1.45 at 980 nm). Then, the UV210 film (*Rohm and Haas*) is deposited by spin-coating leading to 1 µm-thick film, followed by a softbake step to remove the solvent. By way of DUV-lithography (20 mJ/cm^2 at λ_{DUV} = 248 nm), the waveguide pattern defined on a quartz/chromium mask is transferred onto the UV210 guiding layer and followed by a post-exposure bake to cross-link the polymer. Then a development process with a basic developer is necessary to obtain the rib waveguides. The optical structures of family 2 are re-exposed to the DUV light source: four samples have been made with post-development irradiation doses of 0.02, 5, 10 and 15 J/cm^2. Finally, an annealing is carried out for both family structures to stabilize the UV210 material. As a result, scanning electron micrographs (SEM) of 400 nm- and 4 µm-width rib waveguides of family 1 before the annealing step are presented on Fig. 2. These pictures highlight the utilization of an appropriate set of development

This work was supported by Rennes Métropole, Région Bretagne, CNRS and ANR-08-JCJC-0136-01 programs.

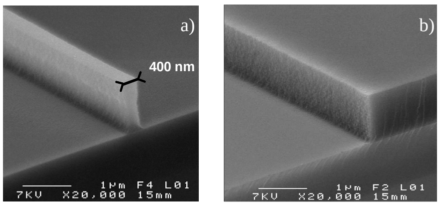

Figure 2. SEM view of rib waveguides of family 1 before the annealing step: a) 400 nm- and b) 4 µm- widths.

parameters: waveguides present low surface roughness and vertical sidewalls, which is important for the achievement of efficient light confinement.

IV. Integrated Optical Characterization and Discussions

A specific optical coupling set up has been developed to characterize optical losses in such UV210 waveguides by using the cut-back method. A laser source operating at λ=980 nm with an enhanced control in temperature is used for the optical injection. The output signal, after propagation through the sample, is monitored with a camera (*Pulmix*) and an optical powermeter (*Ophir* – PD300). First, the detected output optical field characterizes a single-mode propagation with a suitable optical confinement in the core region. The cut-back method is based on the relative measurement of output optical power for different lengths of waveguides that can be expressed as

$$10\log\left(P_{L_1}^{TE-TM} \Big/ P_{L_2}^{TE-TM}\right) = -\alpha^{TE-TM}\,\Delta L \qquad (1)$$

with, $\Delta L = (L_1 - L_2)$ the distance between two respective output cleaved faces, P_{L_1,L_2}^{TE-TM} the optical power measured after propagation at lengths L_1 and L_2 for the TE_{00} and TM_{00} optical modes and α^{TE-TM} the optical propagation losses in dB/cm for each polarization. With this method, optical losses have been evaluated on five rib waveguides (4µm-width and 1µm-height): one of family 1 and four of family 2 (irradiation doses: 0.02, 5, 10 and 15 J/cm^2). As an example, for one sample of family 2 with an irradiation dose of 0.02 J/cm^2, the exit power P has been assessed for four stabilized laser operating currents I and five waveguide lengths (L_1 to L_5), always into a fixed waveguide structure and with the same input cleaved face in order to cancel the variation of injection coupling losses. Considering (1), the quantity $10\log\left(P_{L_5}^{TE-TM} \Big/ P_{L_i}^{TE-TM}\right)$ has been plotted as a function of $(L_i - L_5)$ for TE_{00} mode (Fig. 3a) with L_5 the shortest length and L_i the five studied lengths (i=1 to 5). Then, by fitting the experimental points, we obtain four straight lines, one for each laser operating current. Since such lines almost overlaid, we conclude that propagation losses, obtained from the slopes, are independent of the laser current. Thus, for a 0.02 J/cm^2 irradiated UV210 waveguide, optical losses have been evaluated as 4.0 ± 0.2 dB/cm for TE_{00} polarization and, with the same method, as 7.0 ± 0.2 dB/cm for TM_{00} polarization. The methodology described previously has been applied to all

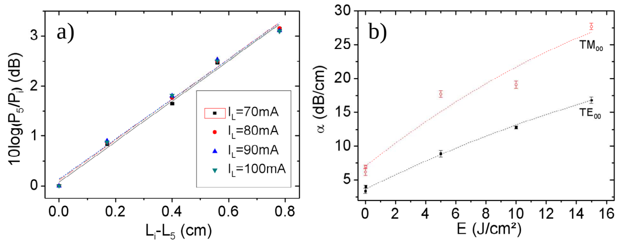

Figure 3. a) $10\log\left(P_{L_5}^{TE} / P_{L_i}^{TE}\right)$ vs. $(L_i - L_5)$ measured on a specific 0.02 J/cm^2 irradiated rib waveguide for TE_{00} mode. b) Propagation losses vs. irradiation dose for both polarizations.

the other samples. For both TE_{00} and TM_{00} modes, Fig. 3b shows the relationship between average propagation losses and irradiation doses. This highlights the increase of propagation losses with the irradiation dose: α^{TE} ranges from 3.4 ± 0.4 dB/cm for an as deposited waveguide to 16.8 ± 0.5 dB/cm for a 15 J/cm^2 irradiated waveguide. In the same way, α^{TM} ranges from 6.2 ± 0.5 dB/cm to 27.7 ± 0.5 dB/cm. This enhancement can be due to the new chemical species produced during DUV-induced transformations, leading to higher absorption at 980 nm.

V. Conclusion

The realization of sub-micronic rib waveguides has been validated by DUV lithography thanks to the UV210 photo-resist. First, this work presents ellipsometric measurements highlighting the refractive index variation as a function of DUV exposure doses on an UV210 film. A large index contrast up to 2.10^{-2} can be achieved between areas either irradiated or unexposed. So as to measure optical losses with the cut-back method, we have realized relevant single-mode TE_{00} and TM_{00} rib waveguides based on UV210 polymer with proper confinement of the optical modes. As a result, unexposed UV210 rib waveguides feature propagation losses α^{TE} = 3.4 ± 0.4 dB/cm and α^{TM} = 6.2 ± 0.5 dB/cm regarding both polarizations. Such properties prove that this photo-resist comes up as a promising material for the realization of sub-wavelength structures in integrated optics. Further works are under investigation to understand and reduce such an increase of optical losses in post-development irradiated waveguides in order to enhance the UV210 optical properties.

References

[1] J. S. Kim, J.W. Kang and J. J. Kim, "Simple and low cost fabrication of thermally stable polymeric multimode waveguides using a UV-curable epoxy," Jpn. J. Appl. Phys., vol. 42, pp. 1277–1279, 2003.

[2] B. Bêche, N. Pelletier, E. Gaviot and J. Zyss, "Single-mode TE_{00}-TM_{00} optical waveguides on SU-8 polymer," Opt. Commun., vol. 230, pp. 91–94, 2004.

[3] P. B. Sahoo, R. Vyas, M. Wadhwa and S. Verma, "Progress in deep-UV photoresists," Bull. Mater. Sci., vol. 25, pp. 553–556, 2002.

[4] W. J. Tomlinson, I. P. Kaminow, E. A. Chandross, R.L.Fork and W. T.Silfvast, "Photoinduced refractive index increase in poly(methylmethacrylate) and its applications," Appl. Phys. Lett., vol. 16, pp. 486–489, 1970.

[5] S. Jagar et al., "A FinFET and Tri-gate MOSFET's channel structure patterning and its influence on the device performance," Thin Solid Films, vol. 462, pp. 1–5, 2004.